

ADSORPTION OF HYDROGEN ON A Pt(111) SURFACE

K. CHRISTMANN, G. ERTL and T. PIGNET

Institut für Physikalische Chemie der Universität, München, W. Germany

Received 6 August 1975; manuscript received in final form 6 October 1975

The $H_2/Pt(111)$ system has been studied with LEED, ELS, thermal desorption spectroscopy and contact potential measurements. At 150 K H_2 was found to adsorb with an initial sticking coefficient of about 0.1, yielding an atomic H:Pt ratio of about 0.8:1 at saturation. H_2/D_2 exchange experiments gave evidence that adsorption is completely dissociative. No extra LEED spots due to adsorbed hydrogen were observed, but the adsorbate was found to strongly damp the secondary Bragg maxima in the I/V spectrum of the specular beam. The primary Bragg maxima were slightly increased in intensity and shifted to somewhat lower energy. A new characteristic electron energy loss at -15.4 eV was recorded upon hydrogen adsorption. The thermal desorption spectra were characterized by a high temperature (β_2 -) state desorbing with second order kinetics below 400 K and a low temperature (β_1 -) state that fills up, in the main, after the first peak saturates. The β_2 -state is associated with an activation energy for desorption E^* of 9.5 kcal/mole. The decrease of E^* with increasing coverage and the formation of the β_1 -state are interpreted in terms of a lateral interaction model. The anomalous structure in the thermal desorption spectra is attributed to domains of non-equilibrium configuration. The work function change $\Delta\phi$ was found to have a small positive maximum (~ 2 mV) at very low hydrogen doses (attributed to structural imperfections) and then to decrease continuously to a value of -230 mV at saturation. The variation of $\Delta\phi$ with coverage is stronger than linear. The isosteric heats of adsorption as derived from adsorption isotherms recorded via $\Delta\phi$ compared well with the results of the analysis of the thermal desorption spectra.

1. Introduction

Platinum is the most important material for the heterogeneous catalysis of hydrogenation reactions. Therefore the interaction of hydrogen with the polycrystalline surface of this metal has been extensively studied in the past. Surprisingly the information on this adsorption system still seems to be rather incomplete and even controversial, for example with respect to the polarity of the adsorption bond [1–6], the binding energy [3,7–10] or (a question which is of still more fundamental importance) if adsorption takes place with dissociation of the H_2 molecule or not [1–3,11]. During the last few years a series of experiments have been performed with single-crystal surfaces [12–21], but, particularly with the most densely packed (111) plane, the picture has remained unclear. Whereas Somorjai and coworkers

[12,21] concluded that hydrogen interacted with low index platinum surfaces only at rather high temperatures, Weinberg and Merrill [13] reported rapid adsorption on Pt(111) at low temperature – and even the formation of an ordered adsorbate structure as detected by LEED. Baldwin and Hudson [14] concluded from their thermal desorption and electron impact desorption studies with Pt(111) that hydrogen adsorbs dissociatively at room temperature up to a coverage of about $\theta = 0.3$. Smith and Palmer [15] observed rapid hydrogen isotope exchange on an epitaxially grown Pt film with (111) orientation. Rye and Lu [16] performed thermal desorption experiments with a Pt(111) surface exposed to H_2 at 125 K and observed a single desorption maximum 330 K. Using H_2 and D_2 these authors reported complete isotopic equilibration [16,17], whereas Bernasek and Somorjai [19] using a molecular-beam technique, were unable to detect any HD formation at all on this low index surface, only on a surface exhibiting a periodic array of atomic steps. During the present study also it became evident that, with the Pt/ H_2 system, structural imperfections of the (111) surface may cause marked variations of the adsorptive properties. Therefore considerable care was taken to work with surfaces which were chemically and structurally as perfect as can be achieved in the present state of the art. Results of measurements performed with stepped surfaces (similar to those described by Somorjai) will be published later.

The experiments were performed by applying a combination of techniques, namely Auger electron spectroscopy (AES), low-energy electron diffraction (LEED) and electron energy loss spectroscopy (ELS) for characterizing the chemical, structural and electronic states of the surface, respectively, work function measurements mainly for evaluating adsorption isotherms and isosteric heats of adsorption, and thermal desorption spectroscopy for determining activation energies for desorption as well as for following the kinetics of ad- and desorption and of the isotopic exchange reaction.

2. Experimental

The sample was prepared by cutting an elliptical slice (area of the front plane 1.1 cm^2 , thickness about 1 mm) from a Pt single crystal by means of spark-erosion after proper orientation ($\pm 0.5^\circ$) by X-ray diffraction. The surface was mechanically polished and briefly etched in hot aqua regia prior to spot-welding the sample between two parallel-running thin tungsten wires fixed to two Cu blocks mounted on the crystal manipulator. The temperature could be measured to within $\pm 1^\circ\text{C}$ by means of a chromel–alumel thermocouple spot welded to the backside of the crystal. The sample could be cooled down to 150 K using liquid nitrogen.

The experiments were performed within a commercial stainless-steel UHV system (Varian) with a base pressure of 10^{-8} Pa ($\sim 10^{-10} \text{ Torr}$), the main component of the residual gas being helium. It was found to be of very great importance to keep the partial pressure of CO always below 10^{-9} Pa in order to obtain reproduc-

ble results and to prevent any detectable contamination of the surface. The apparatus was equipped with four-grid LEED optics including a moveable Faraday cup for measuring LEED intensities and with an additional glancing angle electron gun for AES. The beam current of the latter was kept below $5 \mu\text{A}$ in order to minimize interaction effects with the surface. The composition of the residual gas atmosphere, as well as thermal desorption spectra, were recorded with a quadrupole mass spectrometer (Balzers QMG 111). Contact potential measurements were performed by the self-compensating vibrating condenser method [22] using oxidized tantalum as material for the reference electrode and by the diode technique [23]. Both methods yielded identical results to within a few meV. The work function data reported here were obtained with the diode method using a thoriated tungsten filament whose temperature was kept below 1000 K in order to prevent decomposition of the molecular hydrogen. By maintaining the electron emission current between the filament and the sample surface constant, variations of the work function could be recorded directly on an $x-t$ plotter [24], with an accuracy of ± 0.5 meV, the long-time stability being about ± 5 meV/h. Details of this device will be published elsewhere [25].

High purity gases (H_2 : 99.99%; D_2 : 99.95%) were admitted to the vacuum system through bakeable leak valves. The total pressure was measured with a Bayard–Alpert ionization gauge which was also used for calibrating the quadrupole mass spectrometer, taking into account the manufacturer's correction factor for hydrogen.

After mounting the sample in the UHV system and achieving the base pressure, the surface was cleaned by prolonged argon ion bombardment (energy 600 eV) and annealing (1400 K) cycles. The main surface contaminants were the elements S, Si, P and C. No attempt was made to clean the surface by an oxidation/reduction procedure [26], since it was found that admission of oxygen to the system always increased the CO partial pressure. The LEED pattern of a clean Pt(111) was characterized by the appearance of sharp diffraction spots from the (unreconstructed) substrate lattice (see below), whereas the presence of larger amounts of Si or P impurities caused the formation of rather complex surface structures. The Auger electron spectrum from the clean Pt(111) surface was found to be identical to that published recently by Bernasek and Somorjai [19] and is therefore not reproduced here.

Reproducibility of the contact potential data proved to be a much more sensitive indicator of the state of surface cleanliness than AES, a fact previously observed with the system H_2/Ni [27].

3. Results

3.1. LEED

Fig. 1 shows a LEED pattern from a clean and well-annealed Pt(111) surface.



Fig. 1. LEED pattern of a clean Pt(111) surface, electron energy 56 eV.

Very sharp diffraction spots from the substrate lattice and a rather low background intensity indicate a high degree of perfection in the periodicity of the surface lattice. Weinberg and Merrill [13] reported the formation of a "transient" 2×2 superstructure after admission of hydrogen to a Pt(111) surface which, however, could not be reproduced in the same laboratory [28]. Likewise in the present work all attempts to observe 'extra' LEED spots due to adsorbed hydrogen, in any range of coverage or temperature down to 150 K, failed.

The variation in the intensity of the specularly reflected (0,0) beam with electron energy, recorded with a clean Pt(111) surface at an angle of incidence of $5(\pm 1)^\circ$ and at a temperature of 150 K, is shown in fig. 2 (full line). The characteristic features of this I/V curve are qualitatively the same as those reported by Smith and Merrill [18], apart from the fact that due mainly to the low temperature in the present case, the intensities are considerably higher. According to the simple kinematic diffraction theory the energies of the primary Bragg maxima should be given by the formula [29]

$$V_B = \left(\frac{l}{d}\right)^2 \frac{150.4}{4 \cos^2 \varphi} - V_{in} \quad (1)$$

where l denotes the order of diffraction, d the interlayer spacing perpendicular to the surface, φ the diffraction angle, and V_{in} the inner potential. Provided that the kinematic approximation is applicable, a plot of V_B versus l^2 therefore should yield a straight line. In fig. 3 we see that this is indeed the result. From the slope a lattice constant for the surface region $a_{0,surf} = 3.91 (\pm 0.02) \text{ \AA}$ is evaluated which agrees within the limits of error with the bulk value ($a_{0,bulk} = 3.924 \text{ \AA}$). A mean value $V_{in} \approx 12 \text{ eV}$

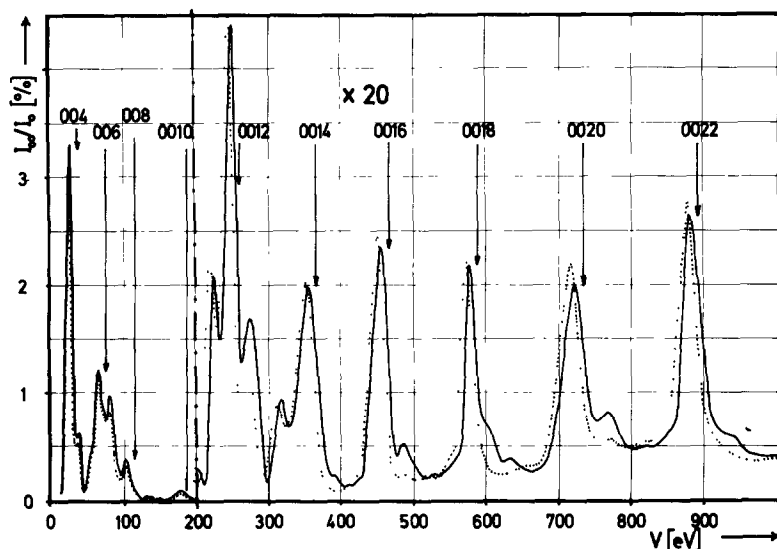


Fig. 2. Intensity/voltage (I/V) curve for the (0,0) beam from a clean (full line) and a hydrogen saturated Pt(111) surface (dotted line).

for the inner potential follows from the intersection of the straight line with the ordinate axis. The value of $a_{\text{surf}} = 3.91 \text{ \AA}$, of course, does not refer to topmost atomic layers only.

Strong secondary Bragg maxima (fig. 2) and systematic deviations of the mean inner potential from the average value (fig. 3) in the energy range below 200 eV clearly show the weakness of the kinematic approximation underlying our evaluation of a_{surf} in this range. On the other hand, the escape depth of slow electrons with energies less than 500 eV does not extend to more than 10 \AA , so that we can be rather sure that they yield information from the surface region.

The dotted line in fig. 2 represents the LEED spectrum of the specular beam after saturation of the surface with hydrogen at 150 K. The result is some shifting of the positions of the primary Bragg maxima toward somewhat lower energies, this effect being most pronounced with the 0014 Bragg maximum ($\sim 7.5 \text{ eV}$). In the energy range above 200 eV the intensity of the primary Bragg peaks is slightly increased whereas most of the features characterizing secondary Bragg maxima are strongly damped in intensity. Surprisingly, these effects are much less pronounced in the lower energy range, where dynamic scattering events are expected to dominate.

3.2. Electron loss spectroscopy

The analysis of the energy distribution of secondary electrons excited by a mono-

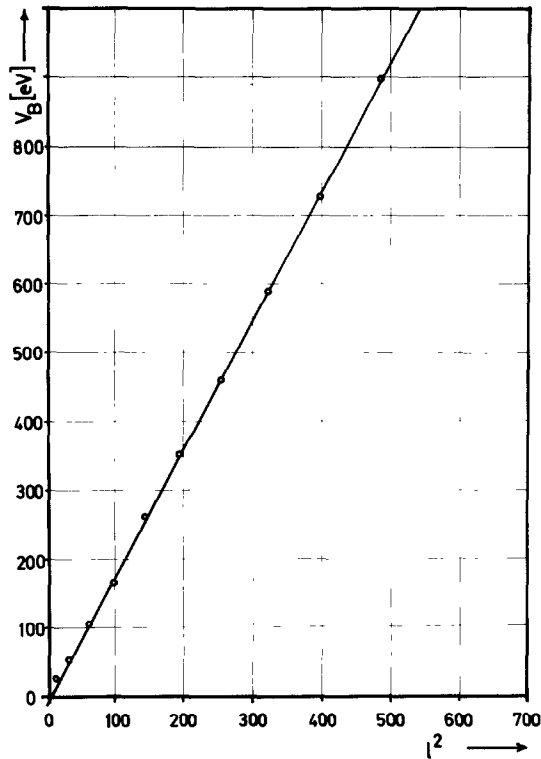


Fig. 3. Plot of the energies of the primary Bragg maxima (001) versus l^2 [see eq. (1)] for a clean Pt(111) surface.

energetic primary electron beam can be performed simply, using the LEED optics as a retarding field energy analyzer, and yields information on characteristic energy losses of the solid (e.g. interband and intraband transitions, plasmon excitations) as well as on single-electron excitations involving chemisorption levels [30,31].

Electron loss measurements with a clean Pt(111) surface have been made previously by Hölzl et al. [30]. These authors published an energy distribution curve for a primary energy of 300 eV whose qualitative features agree well with the results of the present work (taken at $E_p = 200$ eV), reproduced in fig. 4. Following Hölzl the peaks a ($\Delta E = 5.2$ eV) and b (11.7 eV) are attributed to interband transitions, whereas c (22.2 eV) and d (30.4 eV) are interpreted as surface and volume plasmon losses, respectively.

The second curve drawn in fig. 4 was recorded after completely covering the surface with adsorbed hydrogen. The peaks a and c remain nearly unchanged whereas peak b is strongly damped and peak d is somewhat shifted towards the elastic peak. This result raises some doubt as to the validity of the original assignment [32] of

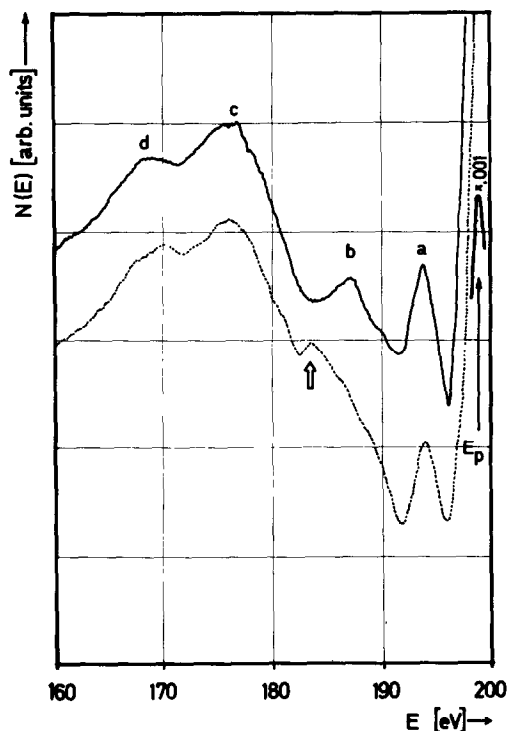


Fig. 4. Energy distribution of electrons backscattered from Pt(111). Primary energy $E_p = 199.2$ eV; full line: clean, dashed line: H_2 covered surface; for a, b, c, d, see text.

these peaks. The most interesting feature in the present work, however, is the appearance of a new characteristic energy loss (indicated in fig. 4 by an arrow) at -15.4 eV. Quite similar chemisorption-induced energy losses were observed previously with the systems Ni(110)/ H_2 (15 eV) [30] and Ni(100)/ H_2 [27].

3.3. Thermal desorption spectroscopy

Thermal desorption spectra from hydrogen covered Pt(111) surfaces have been reported previously by Baldwin and Hudson [14] and by Lu and Rye [17]. However, in both case, without any in situ monitoring of the chemical and crystallographic state of the surface with AES and LEED. Baldwin and Hudson [14] exposed their sample to hydrogen at room temperature and observed a single desorption peak with its maximum at about 470 K, whereas Lu and Rye started at a temperature of 125 K and reported a single desorption peak at high exposures also, but around 330 K. They determined an activation energy for desorption of 17.5 kcal/mole.

In the present work it was found that the heat of adsorption of hydrogen on a clean and well-annealed Pt(111) surface attains rather low values and it was necessary to perform the adsorption prior to thermal desorption at the lowest attainable temperatures. The desorption spectra presented here were started at 150 K, but still we cannot exclude the possibility that, at high coverages, a small part of the adsorbed hydrogen is pumped off the surface during the evacuation of the system prior to applying the temperature program to the sample.

A series of thermal desorption spectra taken after different exposures is reproduced in fig. 5. These spectra are characterized by a maximum growing up at 390 K at small coverages and shifting towards lower temperatures with increasing exposure. This state (which will be denoted by β_2) appears to be related to the single desorption peak reported by Lu and Rye [17], although the derivation of the activation energy for desorption leads to a rather different result. This β_2 -peak is associated with a shoulder at the low-temperature side which increases with increasing exposure after completion of the β_2 -state, thus indicating the filling of a second state (β_1) which starts to desorb near the lowest attainable temperatures in the present experiments (150 K). Contributions from the backside of the crystal were found to be negligible by control experiments in which the backside was covered by an evaporated gold layer.

If the effective pumping speed of the vacuum system S_{eff} is high enough (a condition fulfilled in the present experiments) then the desorbing amount n (molecules/cm²) may be evaluated from the area $\int p \, dt$ below the corresponding thermal desorption trace through the equation

$$n = \left(\frac{S_{\text{eff}}}{A k T_g} \right) \int p \, dt, \quad (2)$$

where A is the area of the surface and T_g the gas phase temperature. S_{eff} was obtained from the relation $S_{\text{eff}} = V/\tau$, where V is the volume of the vacuum chamber and τ the time constant for its evacuation. For our system, and for H₂, $S_{\text{eff}} = 900 \pm 150$ l/sec. Unfortunately due to the uncertainty in the parameters of eq. (2) a rather high degree of uncertainty ($\pm 30\%$) is connected with n , the *absolute* amount of desorbing hydrogen molecules. However, the *relative* degree of coverage, $\theta = n/n_{\text{max}}$, may be evaluated from the thermal desorption spectra with much higher accuracy.

An exposure of about 200 L H₂ at 150 K was sufficient to saturate the surface with adsorbed hydrogen. By using eq. (2) the maximum number of adsorbed particles (under the chosen conditions) was estimated to be $6(\pm 2) \times 10^{14}$ molecules/cm². As will be shown later there is strong evidence that all adsorbed particles are in the atomic state. This coverage therefore corresponds to $1.2(\pm 0.4) \times 10^{15}$ H atoms/cm² or, since the (111) plane contains 1.5×10^{15} surface atoms, to an atomic ratio H:Pt of 0.8:1. It can be assumed that still lower adsorption temperatures (or higher pressures) would lead to a further increase of the coverage (by

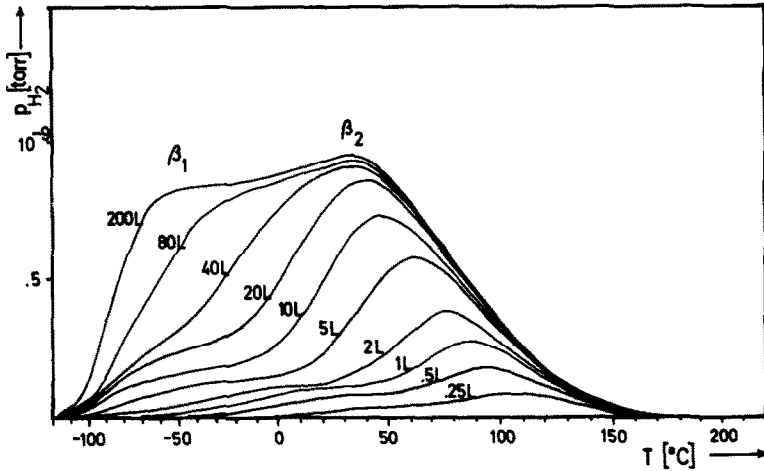


Fig. 5. Set of flash desorption spectra for $H_2/Pt(111)$.

chemisorbed hydrogen) so that an atomic ratio of 1:1 eventually would be reached, as always assumed in 'titration' techniques for determining the number of exposed Pt atoms in dispersed catalysts [33].

The simplest phenomenological rate law for desorption from a single adsorption state may be expressed as

$$-dn/dt = \nu(n) \exp[-E^*(n)/RT] n^x, \quad (3)$$

where ν and E^* , the pre-exponential and desorption activation energy, respectively, are coverage-dependent. The process occurs with reaction order x .

For second-order desorption, and with ν and E^* independent of coverage, the temperature T_{\max} of the peak maximum shifts to lower values with increasing initial coverage. As this clearly occurs with the peak designated β_2 in fig. 5, it is worthwhile to obtain an estimate of E^* for this state by the simple approach of Redhead [34]. When these conditions hold the relationship between T_{\max} and the kinetic parameters is

$$\frac{E^*}{RT_{\max}^2} = \frac{n_{\max}\nu}{(dT/dt)} \exp\left(\frac{-E^*}{RT_{\max}}\right), \quad (4)$$

where

$$n_{\max} = \frac{S_{\text{eff}}}{AkT_g} \int_{t_{\max}}^{\infty} p dt$$

and dT/dt is the (linear) heating rate imposed. The linear plot (fig. 6) of $\ln(n_{\max} T_{\max}^2)$ versus $1/T$ yields from the slope E^*/R , a value $E^* = 9.4$ kcal/mole. Since the

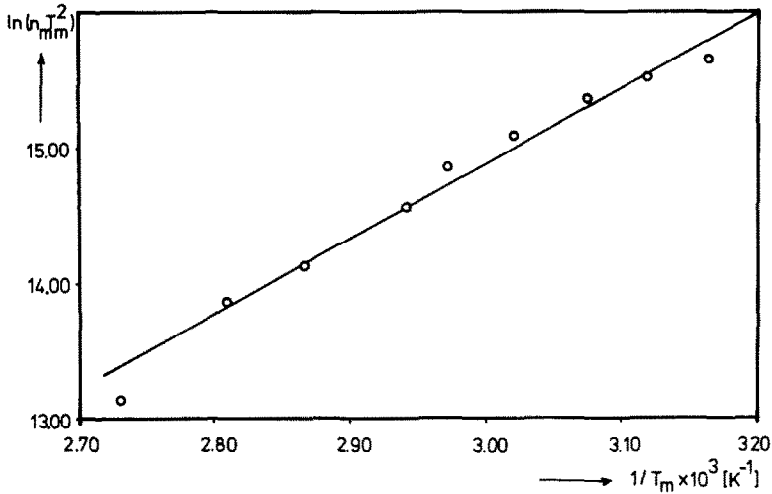


Fig. 6. Second order plot of $\ln(n_{\max} T_m^2)$ versus T_m^{-1} according to Redhead [34].

peak temperature of the β_1 -state is about 100 K lower than that for the saturated β_2 -state, a desorption energy about 3 kcal/mole lower can be estimated for β_1 .

A complete set of thermal desorption spectra, however, contains a great deal of information that is largely ignored in the simple method of Redhead. In fact, at each point (P, t) on a flash desorption trace one can assign a value for the rate of desorption (proportional to P at that point for high pumping speed systems) and a value for the adsorbate concentration, proportional to

$$\int_t^{\infty} P(t') dt'.$$

At any given point along the abscissa (i.e. at a fixed temperature), and with a sufficient number of traces representing the lowest doses on up to saturation, one can then replot the raw data as rate of desorption versus coverage at constant surface temperature. Repeating this for a full set of temperatures spanning the range of the desorption program, one obtains a set of desorption rate isotherms from which, by interpolation, it is possible to extract E^* as a function of coverage. $\nu(n)$ may also be extracted, after assuming a reaction order, but a large relative error will be associated with this parameter unless very accurate determinations of absolute coverage are made (see, for example, refs. [35,36]).

This approach (which is readily programmed to the computer) is independent of any specific model assumptions as to the order of desorption or functional dependence of E^* and ν on coverage, i.e. it is applicable to the general rate law, eq. (3). However, eq. (3) does imply a single-state, lateral interaction model, and this may

not adequately describe many adsorption systems. When the data of fig.5 were subjected to this kind of analysis, the single state assumption was found to be wanting as the final Arrhenius plots displayed totally unsatisfactory curvature. Only the small amount of data available at the high temperature end of the spectra (corresponding to desorption from the tighter-bound β_2 -state and relative coverages below ~ 0.3) yielded E^* values comparable to the heat of adsorption obtained from the equilibrium work function change data (and the 9.4 kcal estimate for the β_2 -state obtained above).

Assuming, then, that the spectra of fig. 5 represent the composite effects of desorption from two independent adsorption states, recourse was had to non-linear curve-fitting techniques to simulate the spectra. From the qualitative shift of the spectra with increasing initial coverage, and the fact that the isotope exchange experiments (section 3.6) indicated adsorption as atoms in both states, second-order desorption was assumed for both states. The simplest 2-state model, namely

$$-dn/dt = A_1 n_1^2 \exp(-E_1^*/RT) + A_2 n_2^2 \exp(-E_2^*/RT), \quad (5)$$

with coverage-independent parameters, simulated any given desorption trace with very little error. The assumption of coverage-independence is probably unrealistic, but the variation from trace to trace in the "best fit" E^* values was found to be relatively small and, moreover, in correspondence with the work function change results.

This model also assumes that the two states desorb independently during the course of the desorption program and some experiments were run to test this as-

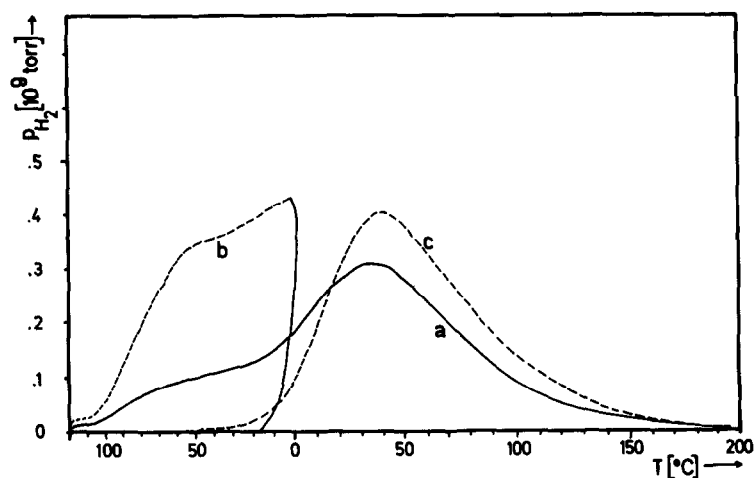
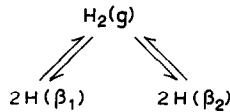


Fig. 7. Thermal desorption curves demonstrating "history": (a) normal dosing procedure (20 L H_2); (b) saturated surface flashed only to 273 K, cooled then; (c) re-flashed to completion.

sumption: Exposing a clean surface at 150 K to ~ 20 L H_2 resulted in the thermal desorption spectrum curve a in fig. 7, i.e. mainly a β_2 -peak but with some contribution from the β_1 -state. When, however, a surface saturated with adsorbed hydrogen was first flashed to ~ 270 K (corresponding, roughly, to the desorption of the β_1 -state, curve b in fig. 7) recooled to 150 K in vacuo, and subsequently re-flashed to completion, the spectrum of curve c, fig. 7, was recorded. The conditions were so chosen that the areas below curves a and c, and hence the initial coverages, were equal. The shapes of the two curves differ considerably, notably in the fact that the β_1 -state is completely absent in trace c. The conclusion is that curve c represents an initial state nearer thermodynamic equilibrium than that of curve a, where adsorption into the β_1 -state proceeds before complete filling of the tighter-bound β_2 -state. Restricted mobility of the adsorbed particles (at least in the low-temperature range of the desorption program) is strongly indicated.

Consequently the desorption process was modeled by eq. (5); two uncorrelated surface states desorbing independently via second-order kinetics with no coverage dependence of kinetic parameters:



Parameters to be fitted: 2 desorption activation energies, 2 pre-exponentials (arbitrary units), 1 distribution coefficient, α , relating the initial relative coverage in the 2 states, given the initial total coverage θ_T :

$$\theta_T = \alpha \theta_{\beta_1} + (1 - \alpha) \theta_{\beta_2},$$

where θ_{β_1} = fractional coverage in state β_1 , $0 \leq \theta_{\beta_1} \leq 1$, and θ_{β_2} = fractional coverage in state β_2 , $0 \leq \theta_{\beta_2} \leq 1$.

Typical spectra spanning the coverage range are shown in fig. 8 along with the fitted curves. Table 1 contains the results of the analysis of these three spectra.

Table 1

θ_T	α	E_1^4 (kcal/mole)	E_2^4 (kcal/mole)
0.15	0.04	4.9	9.1
0.50	0.14	5.5	7.7
0.95	0.37	5.1	6.6

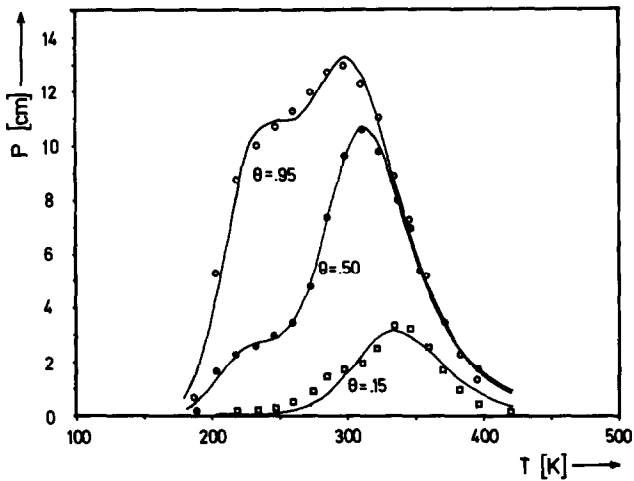


Fig. 8. Computer simulation of assumed 2-state flash desorption spectra at different coverages θ ; — calculated curve; ●, ○, □ experimental data points.

3.4. Contact potential measurements

To our knowledge no measurements with Pt single crystal surface on the variation of the work function by adsorption of hydrogen are reported in the literature, but only data for polycrystalline surface [1–6]. In his pioneering work with the vibrating condenser method Mignolet [1] observed, after exposing platinum at 77 K to H_2 , an increase of the work function which passed through a maximum at +0.10 eV and then decreased to a value of -0.23 eV. Qualitatively similar results were obtained by Sachtler [4] and by Gomer [3] using field electron emission from Pt tips. The general conclusion was to identify the electronegative species (exhibiting a somewhat higher binding energy) with atomically adsorbed hydrogen and the species which lowers the work function with non-dissociatively adsorbed H_2 molecules. As will be shown, this interpretation can no longer be held on the basis of the present results.

Exposing a clean and well-annealed Pt(111) surface to hydrogen leads at first to a very small *increase* of the work function by only 2 mV which is followed by a continuous *decrease* to a final value of -230 meV at 150 K, 1.3×10^{-2} Pa (10^{-4} Torr). As will be discussed in more detail in section 3.7, there is strong evidence that the observed increase of φ is related to residual structural imperfections of the (111) plane. We infer then that hydrogen adsorption on a perfect (111) surface decreases the work function monotonically. The observed value of $\Delta\varphi_{\text{sat}} = -230$ meV is in remarkably good agreement with the data reported by Mignolet [1] for adsorption on evaporated Pt films and also in reasonable agreement with the results of field emission measurements [2,3].

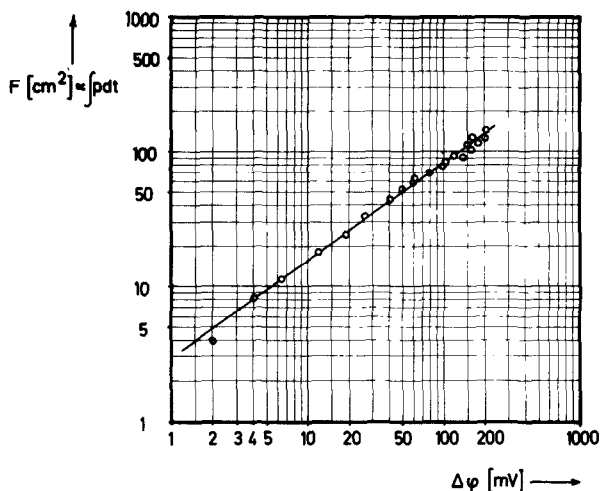


Fig. 9. Double logarithmic plot of the work function change $\Delta\phi$ for $\text{H}_2/\text{Pt}(111)$ against the relative adsorbed amount. The slope is 0.75.

The work function change $\Delta\phi$ was calibrated against the relative coverage by determining the area $\int p dt$ below the corresponding thermal desorption spectrum. The correlation is presented in the form of a double-logarithmic plot in fig. 9. In contrast to similar measurements with hydrogen adsorbed on Ni [27] and Pd [37] single crystal surfaces, $\Delta\phi$ here is not directly proportional to θ (even in the low coverage range). The dependence may be described by the relation

$$\Delta\phi = -0.23 \times \theta^{1.33} \text{ (eV)}. \quad (6)$$

This shows that $\Delta\phi$ varies stronger than linearly with the coverage, a rather surprising result. There is apparently no change in polarity or even a discontinuity in the dipole moment associated with the formation of the β_1 -state after completion of the β_2 -state. $\Delta\phi$ appeared to be only a function of θ and not (within the limits of estimate) of T . Since hydrogen adsorption was found to be completely reversible $\Delta\phi$ could be used as a measure of the adsorbed amount under equilibrium conditions at fixed temperature and pressure. A set of adsorption isotherms constructed by applying eq. (6) to the measured $\Delta\phi$ values is shown in fig. 10. The experiments were performed by varying the temperature of the sample stepwise at fixed pressure and simultaneously monitoring the work function change until the new equilibrium was reached. As an example of this type of measurement a recorder plot for $p = 4 \times 10^{-6}$ Pa (3×10^{-8} Torr), over a temperature range between 150 and 400 K, is reproduced in fig. 11.

From the adsorption isotherms the differential isosteric heat of adsorption $E_{\text{ad}}(\theta)$ may be determined by applying the Clausius–Clapeyron equation,

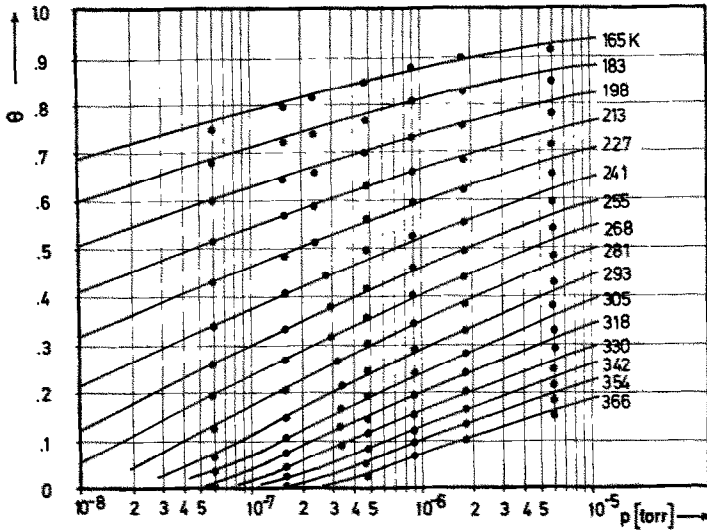


Fig. 10. Adsorption isotherms constructed from $\Delta\varphi$ data, θ_T versus pressure for $H_2/Pt(111)$.

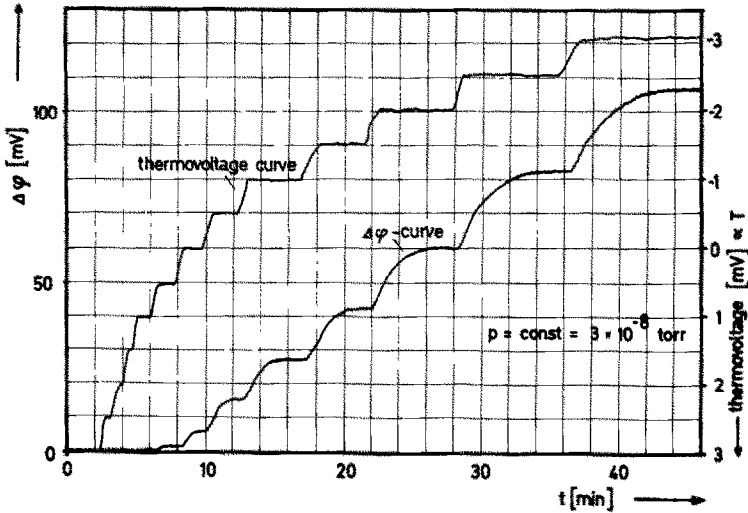


Fig. 11. Typical experimental data run: $\Delta\varphi$ (time) at constant H_2 pressure $P_{H_2} = 3 \times 10^{-8}$ torr; $T_s = 150$ K.

$$\left. \frac{d \ln p}{d(1/T)} \right|_{\theta = \text{const.}} = -\frac{E_{ad}}{R}. \tag{7}$$

The resulting data are plotted in fig. 12 as open circles. Since adsorption takes place with a high rate even at low temperatures it may be concluded that the activation

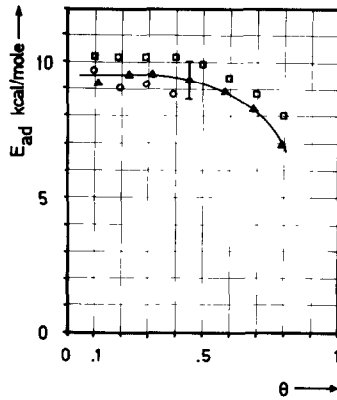
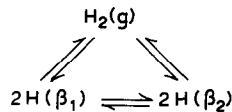


Fig. 12. Adsorption energy E_{ad} as a function of coverage θ (Δ) isotherm data, (\square) computer fit [see eq. (9)], (\circ) TDS data (see section 3.3).

energy for adsorption is negligible. Therefore E_{ad} should be equal to the activation energy for desorption E^* as derived from thermal desorption spectra. Within bounds of perhaps ± 0.5 kcal this appears to be the case (the results of the different methods of analysis are compared in fig. 12). The β_2 -state obviously is associated with a constant adsorption energy of about 9.5 kcal/mole, whereas for coverages $\theta > 0.5$ ($= \beta_1$ -state) the heat of adsorption decreases continuously with increasing surface concentration.

It remains to be seen, though, how well the equilibrium data may be fitted with a simple model – one analogous to the second-order desorption model used in analyzing the TDS data. Again we assume two adsorption states with second-order desorption kinetics. Rye and Lu [16] concluded that H_2 adsorbs on Pt(111) with second-order kinetics, and our evidence (section 3.5) points in this direction also. Then, with equilibrium between all phases,



we obtain the standard Langmuir–Hinshelwood form for fractional coverage in each state,

$$\theta_1 = \frac{(K_1 P)^{1/2}}{1 + (K_1 P)^{1/2}}, \quad \theta_2 = \frac{(K_2 P)^{1/2}}{1 + (K_2 P)^{1/2}},$$

$$K_i = B_i \exp(\Delta H_{ad,i}/RT), \quad (8)$$

with the usual interpretation of the K 's as adsorption equilibrium constants. Experimentally we find $\theta_T \sim \Delta\varphi^{0.75}$. Hence our explicit model relating $\Delta\varphi$, tem-

perature, and pressure is:

$$\Delta\varphi^{0.75} = \frac{A_1 (K_1 P)^{1/2}}{1 + (K_1 P)^{1/2}} + \frac{A_2 (K_2 P)^{1/2}}{1 + (K_2 P)^{1/2}} \quad (9)$$

A_1 and A_2 are constants of proportionality lumping the individual effects of each state on the measured work function and the distribution of total adsorption sites between the two states.

When the full set of isotherm data in fig. 10 was fitted to this model, the following parameter values were obtained for $\Delta\varphi$ [=] mV, P [=] Torr:

$$\begin{aligned} A_1 &= 24.2, & A_2 &= 37.2, \\ B_1 &= 2.25 \times 10^{-3}, & B_2 &= 0.013, \\ \Delta H_{ad,1} &= 8.4 \text{ kcal/mole}, & \Delta H_{ad,2} &= 10.4 \text{ kcal/mole}. \end{aligned}$$

The standard error of the fit (107 residuals) was 4.6 mV and that for each of the heats of adsorption less than 0.4 kcal/mole.

Though no assumption of the variation of the individual heats of adsorption with coverage was made, this model clearly implies a variation in the "average" heat of adsorption one would obtain by the straightforward interpolation procedure and eq. (7). Furthermore, extracting such Clausius–Clapeyron values from the explicit model above, we find them, as expected, bracketing the real values until these begin to fall off more rapidly at the highest coverages. The model yields average values between 10.4 kcal (β_2) at low coverages and 8.4 kcal (β_1) at high.

3.5. Kinetics of adsorption

The rate of adsorption per cm^2 of surface of particles of mass m at a partial pressure p may be written as

$$r_{ad} = \frac{dn}{dt} = s(\theta) \frac{p}{(2\pi mkT)^{1/2}} = s_0 f(\theta) \frac{p}{(2\pi mkT)^{1/2}}, \quad (10)$$

where $s(\theta)$ denotes the sticking coefficient at coverage θ and s_0 the magnitude of this quantity extrapolated to zero coverage. If the rate of desorption may not be neglected an "apparent" sticking coefficient $s_{app} = (r_{ad} - r_{des})/z$, with $z = p/(2\pi mkT)^{1/2}$, will be measured which is smaller than the quantity s describing the adsorption kinetics alone. Reports on s_0 in the literature differ considerably: With polycrystalline Pt surfaces a group of papers reports on values for s_0 between 0.10 and 0.16 [9,38,39], whereas Procop and Völter [7] obtained a much lower value of 0.0045. With a Pt(111) surface Lampton [28] arrived at an apparent $s_0 = 0.08$ at 320 K, a value which is expected to be still higher at lower temperatures as desorption interferes strongly above room temperature. On the other hand Rye and Lu [16] estimated s_0 on Pt(111), at lower temperatures, to have the much lower value of 0.016, and the work of Lang et al. [12] indicate no measureable rate of

hydrogen adsorption at all.

This latter conclusion is in clear disagreement with the present results, but we believe that the findings of Lang et al. [12] are obscured by the fact that these measurements were always performed above room temperature. As discussed in the preceding chapters, under those conditions hydrogen rapidly desorbs from a Pt(111) surface so that the net rate of uptake becomes essentially zero. Similar arguments might hold for the interpretation of the H_2/D_2 exchange measurements by Bernasek and Somorjai [19].

According to eq. (10), $s(\theta)$ may be determined from the slope of $n(t)$ at fixed pressure. $n(t)$ was determined by following $\Delta\varphi(t)$ and using the calibration [eq. (6)] to convert the work function into coverage data, as well as by evaluating the adsorbed amounts from the areas below the thermal desorption spectra as a function of coverage. The resulting values for $s(\theta)$ at 150 K are given in fig. 13. The absolute scale for $s(\theta)$ is accurate only within $\pm 30\%$ (due to the uncertainty in determining absolute quantities of adsorbed particles), whereas the relative values, i.e. $s^* = s(\theta)/s_0$, are much more accurately determined. s_0 turns out to be about 0.10.

Although no extensive measurements at different temperatures were made, the

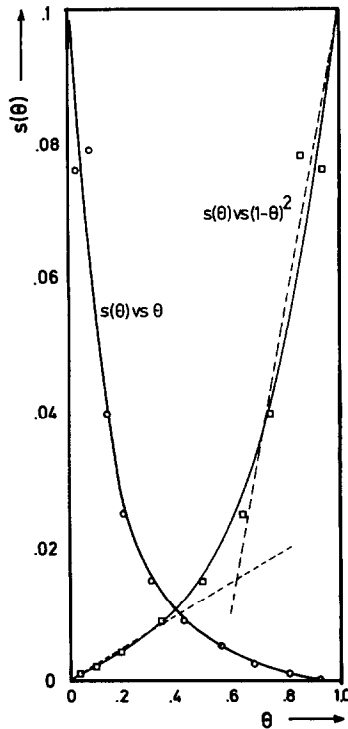


Fig. 13. Sticking coefficient for $H_2/Pt(111)$: $s(\theta)$ versus θ and $s(\theta)$ versus $(1 - \theta)^2$.

general observation was that s_0 was not significantly dependent on temperature as long as desorption can be neglected. This agrees with the careful measurements on polycrystalline Pt wires by Norton and Richards [38], who determined $s_0 = 0.16$, independent of temperature between 77 and 170 K. It is thus concluded that adsorption proceeds without any measurable activation energy. As a consequence the activation energy for desorption should be equal to the (thermodynamic) energy of adsorption as the collective results of fig. 12 suggest.

Some evidence for second-order adsorption kinetics (a conclusion also reached by Rye and Lu [16] in their experiments with Pt(111)) is given by the plot of the sticking coefficient versus $(1 - \theta)^2$ in fig. 13. The curve may be interpreted as being composed of two straight lines corresponding to adsorption into the β_1 - and β_1 -states, respectively.

3.6. Isotopic exchange reaction

A series of measurements was performed using H_2 and D_2 , mainly to clarify the nature of the adsorbed species (i.e. whether it is in an atomic or a molecular state). Although the isotopic exchange reaction was not studied in detail some additional observations were made. Reports on this reaction on polycrystalline [38,39] as well as on single-crystal Pt surfaces [16,17,19] can be found in the literature.

In a series of experiments the clean Pt(111) surface was exposed simultaneously to equal fluxes of H_2 and D_2 . Subsequently thermal desorption spectra for $m/e = 3$ (= HD) were recorded. As can be seen from fig. 14 the shapes of these curves

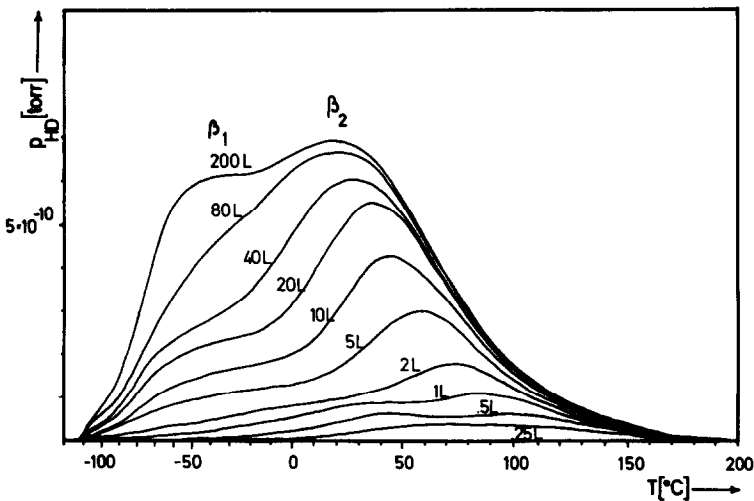


Fig. 14. Set of TDS spectra for HD, the experimental condition being similar to those underlying fig. 5. Dosing data refer to a mixed dose $H_2 : D_2 = 1 : 1$.

are essentially identical to those of fig. 5, particularly with regard to the weakly bound β_1 -state. It is concluded that in both states of adsorption complete equilibration of the hydrogen isotopes takes place which, in turn, can best be understood by assuming that complete dissociation of the adsorbed hydrogen molecules takes place. This conclusion appears to be highly probable in view of the additional fact that the adsorption energy as well as the polarity of the adsorbed particles were not found to change discontinuously.

Exposing the Pt surface not simultaneously but sequentially to H_2 and D_2 lead to the following observations: If just the β_2 -state is filled by exposure to H_2 and subsequently the surface saturated by dosing with D_2 the thermal desorption trace again exhibits complete equilibration of the isotopes over the entire spectrum.

Even more surprising was the finding that after saturating the surface completely with H_2 and subsequently dosing with an equal amount of D_2 (at a temperature which is below the onset of thermal desorption) the thermal desorption spectrum again revealed desorption of HD. This can only be explained by some kind of Eley-Rideal mechanism of exchange between chemisorbed H_{ad} and gas-phase D_2 or exchange between H_{ad} and some deuterium species coupled very weakly to the surface.

The steady-state conversion of $H_2 + D_2$ into HD was measured by recording the HD partial pressure in the continuously pumped vacuum system as a function of temperature at fixed H_2 and D_2 partial pressures. The result is shown in fig. 15 as an Arrhenius plot for the temperature range between 150 and 300 K. The activa-

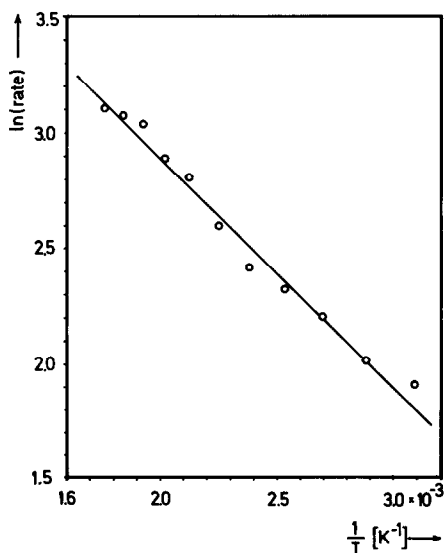


Fig. 15. Arrhenius plot of $\ln(\text{rate})$ versus T^{-1} for the $H_2 - D_2$ isotope exchange reaction. Total conversion rate $< 1\%$.

tion energy is estimated at 2.1 kcal/mole, in fair agreement with the results of similar studies with a Pt(111) surface by Rye and Lu [16,17] who reported a value of 1.2 kcal/mole. With a stepped Pt(111) surface using a molecular beam technique Bernasek and Somorjai [19] determined an activation energy of 4.5 kcal/mole below 600 K, and reported no activity at all with a low index Pt(111) plane. Using a polycrystalline Pt surface below 240 K Norton and Richards [38] obtained an activation energy of 5.8 kcal/mole, this value becoming continuously smaller with temperatures above 240 K.

3.7. Influence of structural imperfections

Early in the course of the present study it became evident that the state of crystallographic perfection might be influencing the results considerably, particularly with respect to the adsorption energy. Some experiments were therefore performed where the surface was not carefully annealed after cleaning by argon ion sputtering. The distortion of the surface periodicity manifested itself in the LEED pattern by the appearance of slightly diffuse (but still bright) diffraction spots from the substrate lattice together with some enhancement of the background intensity. The available experimental technique, however, did not allow a more detailed characterization of the surface imperfection.

The variation of the work function change with hydrogen exposure is reproduced in fig. 16 together with that for a well-annealed surface. $\Delta\varphi$ at first increases by 11 meV and then drops below -300 meV. This effect demonstrates how sensitive-

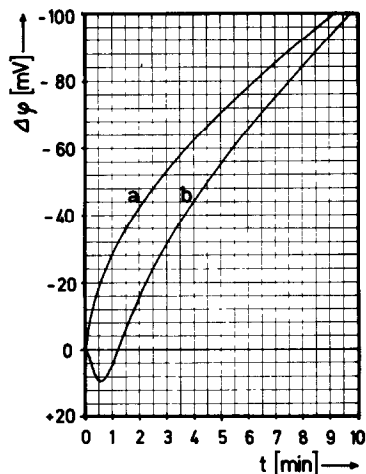


Fig. 16. Effect of degree of crystallographic perfection on work function change measurements. Curve a: $\Delta\varphi(t)$ for a perfect (111) surface. Curve b: $\Delta\varphi(t)$ for a sputtered and unannealed (111) surface.

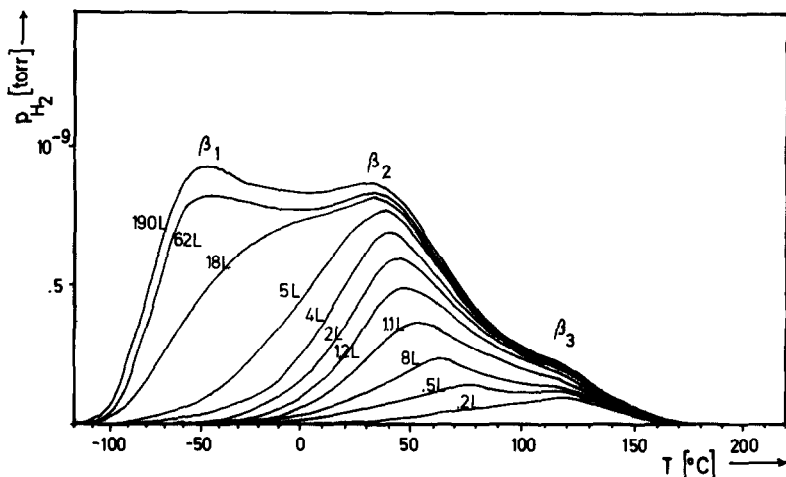


Fig. 17. Set of H_2 TDS spectra for an imperfect Pt(111) surface.

ly $\Delta\varphi$ depends on the surface crystallography and that very careful experiments are necessary in order to get unambiguous and reproducible results. Since, with the distorted surface, the initial work function increase is considerably higher we infer that with a perfect Pt(111) plane $\Delta\varphi$ would be exclusively negative, the rather small increase actually observed being attributed to the presence of residual deviations from the (111) orientation. This effect is being studied in more detail with a periodically stepped Pt(111) surface [40].

A series of thermal desorption spectra from the "imperfect" Pt(111) surface is shown in fig. 17 and is to be compared with the results from the well-annealed surface of fig. 5. The β_1 -state appears now to be more pronounced, i.e. as a real peak, an effect probably correlated with the lower value of $\Delta\varphi$ at saturation (-300 meV instead of -230 meV). Moreover desorption takes place from an additional (β_3 -)state at 380 K, indicating a higher adsorption energy. This state is populated at the lowest hydrogen exposures and was found to be associated with that portion of fig. 16 where $\Delta\varphi$ increases. It is concluded that hydrogen adsorption at structural imperfections takes place with a higher binding energy.

The effect is even more pronounced with the isosteric heat of adsorption evaluated from the adsorption isotherms. Fig. 18 shows a plot of E_{ad} versus $\Delta\varphi$, from which it becomes evident that this quantity increases up to about 16 kcal/mole at low coverages. The shape of this curve is quite similar to that published by Procop and Völter [7] for a polycrystalline Pt surface. Still higher values for E_{ad} , up to 25 kcal/mole at low coverage (on a Pt wire), are reported by Norton and Richards [10].

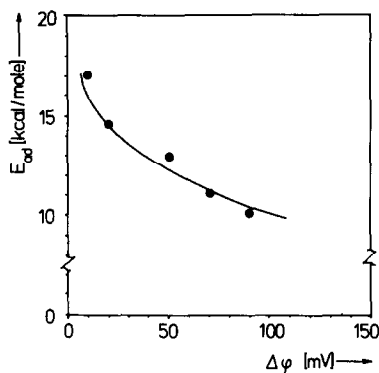


Fig. 18. Adsorption energy (E_{ad}) as a function of $\Delta\phi$, imperfect Pt(111) surface.

4. Discussion

4.1. The nature of the adsorbed particles

The present results demonstrate that hydrogen adsorbs on a low-index Pt(111) surface with an appreciable sticking coefficient and without any measurable activation energy. There is very strong evidence (mainly based on the findings of the isotopic exchange experiments) that, over the whole range of coverage, the adsorbed particles are in the *atomic* state. The conclusion by Bernasek and Somorjai [19] that atomic steps on the platinum surface play a controlling role in dissociating the H_2 molecules is thus not confirmed. Of course the surface under investigation did not exhibit an ideally periodic array of atoms, but from the observation of very sharp LEED spots from the substrate lattice it is concluded that the dimensions of perfectly smooth areas are at least of the order of the coherence width of the slow electrons, i.e. about 100 Å [41].

The adsorption energy (being smaller than 10 kcal/mole H_2) appears to be rather low. If however the dissociation energy of the H_2 molecule is taken into account, the energy for the metal – H bond is found to be about 2.47 eV, comparable with the values for the systems H/Ni(111) (2.73 eV [27]) and H/Pd(111) (2.69 eV [37]). The sign of the work function change is opposite that obtained with Ni or Pd, but in all three the dipole moment is rather small, indicating an essentially covalent chemisorption bond. This is in agreement with recent theoretical treatments of hydrogen adsorption on transition metals [42,43]. According to these theories the formation of a chemisorption level derived from the H 1s-state at 5–6 eV below the Fermi level is predicted. This has been confirmed experimentally, with photoelectron spectroscopy, for Ni and Pd [44], as well as for W [45]. A characteristic energy loss peak with $\Delta E = 15$ eV induced by hydrogen chemisorption was observed in the present case and, previously, with Ni(111) [27]. According to Doyen [43] this

feature is tentatively ascribed to a single-electron excitation from the metallic d-band into the empty 2s-level of the hydrogen atom. The formation of the hydrogen chemisorption bond is predicted to involve the metallic s-electrons to a considerable extent, an effect which may be responsible for the operation of long-range interactions between adsorbed hydrogen atoms. We shall return to this point further on.

The recorded thermal desorption spectra indicate the formation of two different adsorption states with about equal population at saturation, similar to the situation found with hydrogen adsorption on other metals. Several alternative reasons for this effect may be discussed:

(a) The β_1 -state arises from molecular, the β_2 -state from atomic hydrogen, following the interpretation of various authors of the results with polycrystalline platinum [1,3,7]. In the present case this model has to be rejected, mainly on the results of the isotope exchange experiments, which leave little basis for supposing the presence of a molecular adsorbed species anywhere in the coverage range up to saturation. Moreover there is no discontinuous variation of the work function change — which would be expected if there were such a variation of the valence properties of the adsorbate.

(b) The existence of different geometric locations for the H atoms on the surface. The Pt:H ratio at saturation was determined to be smaller than (or at maximum equal to) unity. As each unit cell contains one most favorable adsorption site, then even at saturation there are still sufficient adsorption sites of one kind which may be occupied, without the need for a second (less favourable) type of site. This argument also holds for the two types of adsorption sites proposed by Toya [46] for hydrogen adsorption on metals. According to this model an “r-adatom” is considered as being located outside the electronic surface of the substrate, while the “s-adatom” is some kind of dissolved atom in the metal. As a consequence it would be expected that both species contribute quite differently to the variation of the work function, an effect not observed.

(c) The operation of long-range interactions between adsorbed particles. As was shown theoretically by different authors, indirect (“through-bond”) interactions between adsorbed atoms may come into play if the same metal wave functions are involved in the formation of the chemisorption bond [47–49]. Direct (i.e. through-space) interactions between neighbouring adsorbed hydrogen atoms (arising from orbital overlap or dipole–dipole interactions) may certainly be neglected, since at full coverage their mean distance will be of the order of the lattice constant (2.73 Å), considerably larger than the Bohr radius of hydrogen (0.53 Å), and since the work function change is very small. Grimley and Torrini [49] calculated the indirect interaction between hydrogen atoms adsorbed on neighbouring sites of a W(100) surface to be repulsive with an energy of a few kcal/mole. With the system H/Ni(111) this effect leads to an ordered 2×2 -structure at $\theta = 0.25$ [44], accompanied by a steplike decrease of the isosteric adsorption energy beyond this coverage, i.e. when nearest-neighbour sites start to be filled. Although in the present case no indication for the formation of a superstructure at intermediate coverages was found in the

LEED pattern, a model based on such an 'induced' heterogeneity of the surface appears to be the most probable explanation. According to such a model an H_2 molecule desorbing in the β_2 -state is visualized as being formed by the recombination of two hydrogen atoms with the neighbouring adsorption sites empty, whereas they are occupied in the case of the β_1 -state. Of course this model is rather oversimplified but, as will be shown below, it is able to describe at least qualitatively the essential experimentally-observed features.

Unfortunately no 'extra' LEED spots could be observed, from which we have to conclude that the domains with periodic arrays of hydrogen atoms (if present at all) have dimensions far below the coherence width of the low energy electrons. Since in the case of H/Ni(111) an intense 2×2 LEED pattern could be observed [44], it appears improbable to argue that the scattering amplitude of H_{ad} is too small to yield appreciable intensity in the diffracted beam. [However this effect cannot be completely ruled out since on Pt(111) the H atoms appear to carry less electronic charge than on Ni(111).]

No satisfactory explanation may be offered for the observed changes of the I/V curve from the specular LEED beam (fig. 2). In the case of hydrogen interacting with Pd(111), systematic shifts of the primary Bragg maxima toward lower electron energies were observed. These could be interpreted in terms of a slight (2%) lattice expansion due to partial dissolution of hydrogen [37]. In the present case no systematic correlations between the shifts of the primary Bragg maxima could be found. The solubility of hydrogen in platinum is much lower than in palladium (only about 1 H atom per 10^{11} Pt atoms at 25°C and 1 atm H_2 pressure [50]) and no effects indicating any measurable extent of dissolution could be detected during the adsorption experiments. An expansion of the topmost atomic layers due to partial dissolution of hydrogen therefore appears to be improbable. Similar non-systematic shifts of the energies of the primary Bragg maxima have been found (for example, with sulfur on Ni(100) by Demuth and Rhodin [51]) where appreciable penetration into the lattice certainly can be ruled out. If not due to a layer expansion the observed shifts of the Bragg envelopes might well be due to incorporation of the adsorbed atoms into the outmost atomic layer, but a definite answer can only be expected from a rigorous dynamic analysis of the LEED intensity data.

An even more open problem is that of the non-linear variation of the work-function change with coverage at even the lowest measurable surface concentrations (apart from the small initial positive change which is attributed to the presence of structural imperfections). The fact that $\Delta\phi$ increases stronger than linearly with θ rules out any contribution from depolarization effects due to dipole-dipole interactions. Probably this effect is associated with the long-range interaction between adsorbed hydrogen atoms as discussed above, although the adsorption energy seems not to be affected up to about half the saturation coverage.

4.2. Interpretation of thermal desorption and $\Delta\phi$ data

In the results section it was found that the single-state, lateral-interaction model,

eq. (3), did not adequately account for the TDS data (if the kinetic parameters were assumed to be functions of coverage only, not temperature) and that the 2-state model, eq. (5), simulated the results very well. This does not contradict our proposed atomistic model of the previous section which attributes the development of the β_1 -state to the filling-in of nearest-neighbour sites with a concomitant rise in repulsive interactions. Actually it is implicitly assumed, in eq. 3, that the kinetic parameters are unique functions of coverage and that they "follow" the coverage instantaneously. That is, though $E^*(n)$ is more accurately written $E^*(n - \tau dn/dt)$, we assume that the relaxation time τ is negligible and the adsorbed particles maintain an equilibrium configuration throughout the course of the desorption program. The question of whether or not this assumption is fulfilled is of some importance when the method fails to yield satisfactory results. Failure could be due simply to desorption from more than one independent adsorption 'state', in which case eq. (3) would no longer apply, or to failure of the adsorbate to maintain configurational equilibrium the desorption program.

Bauer et al. [36], who have applied the method carefully to a large amount of TDS data from certain metal-on-metal adsorption systems, judge the feasibility of the technique for multiple-peak spectra by the quality of the final results, presumably the linearity of the ultimate Arrhenius plots and the regularity of the parameter variation. When it is found to be unsatisfactory by these criteria they judge the reason to be the existence of multiple states. However, Adams [52] has shown, assuming configurational equilibrium, that lateral interactions alone can cause such multiple-peak character in TDS. Undoubtedly non-equilibrium effects can add even more structure to the spectra. Moreover, in this case, the distinction between the multiple-state and lateral interaction models becomes quite blurred. For example, if a significant fraction of the adsorbed particles maintain domains of a specific non-equilibrium configuration (in which lateral interactions may be more pronounced), the desorption spectra will have "2-state" character in the sense that a 2-state model will simulate the data better. This appears to be the case for the $H_2/Pt(111)$ system as we have observed non-equilibrium adsorption at the low dosing temperatures employed, and non-equilibrium may be maintained for some time into the desorption program.

The $\Delta\varphi$ measurements, on the other hand, very likely yielded true equilibrium data as most of this data was taken at higher temperatures and longer times were employed (the approach to steady-state was carefully monitored). We see from the results, then, that a 2–3 kcal/mole difference in binding energy between "states" β_1 and β_2 is quite sufficient to ensure virtually the complete filling of β_2 before any appreciable uptake into β_1 (at equilibrium). It is thus satisfying to observe an essentially constant isosteric heat of adsorption below about 0.5 fractional coverage. The two-state equilibrium model of eqs. (8) and (9) is also consistent with our atomistic proposals of section 4.1. The fraction of adsorbate in the β_1 -state is considered to be just that fraction of the total experiencing nearest-neighbour repulsion. This simple view appears to hold up rather well until the highest coverages, when the heat of adsorption falls off more rapidly than predicted. In later work we shall apply the lateral interaction model in greater detail to the hydrogen/platinum system [40].

5. Summary and conclusions

Hydrogen has been found to adsorb dissociatively on Pt(111) with a relatively high sticking coefficient and to reach at least 50% of monolayer coverage at 150 K. The adsorption energy is less than 10 kcal/mole at low coverages and falls continuously for relative coverages over 50% of saturation. The fall-off is attributed to repulsive lateral interactions between adsorbate particles.

Many aspects of this important adsorption system need more detailed study, in particular the kinetics of adsorption which may be amenable to analysis in terms of the lateral interaction-model also. The LEED I/V data and the functional dependence of $\Delta\varphi$ on θ are only poorly understood. Clearly the geometric and electronic details of the adsorption bond require further elucidations. Finally, knowledge of the effects of structural imperfections on adsorption properties would be especially valuable in the study of real-world catalysts.

Acknowledgements

Financial support of this work by the Deutsche Forschungsgemeinschaft (SFB 128) is gratefully acknowledged.

References

- [1] J.C.P. Mignolet, *J. Chim. Phys.* 54 (1957) 19.
- [2] R. Suhrmann, G. Wedler and H. Gentsch, *Z. Physik. Chem. NF* 17 (1958) 350.
- [3] R. Lewis and R. Gomer, *Surface Sci.* 17 (1969) 333.
- [4] W.M.H. Sachtler and G.J.H. Dorgelo, *Z. Physik. Chem. NF* 25 (1960) 69.
- [5] W.J.M. Rootsaert, L.L. van Reijen and W.M.H. Sachtler, *J. Catalysis* 1 (1962) 416.
- [6] V. Ponec, *J. Catalysis* 6 (1966) 362.
- [7] M. Procop and J. Völter, *Surface Sci.* 33 (1972) 69.
- [8] J.J. Stephan, V. Ponec and W.M.H. Sachtler, *J. Catalysis* 37 (1975) 81.
- [9] Y. Nishiyama and H. Wise, *J. Catalysis* 32 (1974) 50.
- [10] P.R. Norton and P.J. Richards, *Surface Sci.* 44 (1974) 129.
- [11] W.A. Pliskin and R.P. Eischens, *Z. Physik. Chem. NF* 24 (1960) 11.
- [12] B. Lange, R.W. Joyner and G.A. Somorjai, *Surface Sci.* 30 (1972) 454.
- [13] W.H. Weinberg and R.P. Merrill, *Surface Sci.* 33 (1972) 493.
- [14] V.H. Baldwin and J.B. Hudson, *J. Vacuum Sci. Technol.* 8 (1971) 49.
- [15] J.N. Smith and R.L. Palmer, *J. Chem. Phys.* 56 (1972) 13.
- [16] K.E. Lu and R.R. Rye, *Surface Sci.* 45 (1974) 677.
- [17] K.E. Lu and R.R. Rye, *J. Vacuum Sci. Technol.* 12 (1975) 334.
- [18] D.L. Smith and R.P. Merrill, *J. Chem. Phys.* 53 (1970) 3588.
- [19] S.L. Bernasek and G.A. Somorjai, *J. Chem. Phys.* 62 (1975) 3149.
- [20] G. Kneringer and F.P. Netzer, *Surface Sci.* 51 (1975) 526.
- [21] A.E. Morgan and G.A. Somorjai, *Surface Sci.* 12 (1968) 405.
- [22] G. Ertl and D. Küppers, *Ber. Bunsenges.* 75 (1971) 1017.
- [23] A.G. Knapp, *Surface Sci.* 34 (1973) 289.

- [24] D.J. Klemperer and J.C. Snaith, *J. Phys.* E4 (1971) 860.
- [25] K. Christmann and H. Herz, in preparation.
- [26] W.H. Weinberg, R.M. Lambert, C.M. Comrie and J.W. Linnett, *Surface Sci.* 36 (1972) 299.
- [27] K. Christmann, O. Schober, G. Ertl and M. Neumann, *J. Chem. Phys.* 60 (1974) 4528.
- [28] V.A. Lampton, M.Sc. thesis, Univ. of Calif., Berkeley (1971).
- [29] S. Andersson and B. Kasemo, *Surface Sci.* 25 (1971) 273.
- [30] F. Steinrisser and E.N. Sickafus, *Phys. Rev. Letters* 27 (1971) 992.
- [31] J. Küppers, *Surface Sci.* 36 (1973) 53.
- [32] W. Schröder, E. Peters and J. Hölzl, *Appl. Phys.* 3 (1974) 135.
- [33] J.E. Benson and M. Boudart, *J. Catalysis* 4 (1965) 704.
- [34] P.A. Redhead, *Vacuum* 12 (1962) 203.
- [35] D.A. King, T.E. Madey and J.T. Yates, *J. Chem. Phys.* 55 (1971) 3236; see also: D.A. King, *Surface Sci.* 47 (1975) 384.
- [36] E. Bauer, H. Poppa, G. Todd and F. Bonczek, *J. Appl.* 45 (1974) 5164.
- [37] H. Conrad, G. Ertl and E.E. Latta, *Surface Sci.* 41 (1974) 435.
- [38] P.R. Norton and P.J. Richards, *Surface Sci.* 41 (1974) 293.
- [39] R.J. Breakspere, D.D. Eley and P.R. Norton, *J. Catalysis* 27 (1972) 215.
- [40] K. Christmann, G. Ertl and T. Pignet, in preparation.
- [41] (a) R.L. Park, in: *The Structure and Chemistry of Solid Surface*, Ed. G.A. Somorjai (Wiley, New York, 1969) p. 28–1.
(b) R.L. Park, J.E. Houston and D.G. Schreiner, *Rev. Sci. Instr.* 42 (1971) 60.
- [42] J.R. Smith, S.C. Ying and W. Kohn, *Phys. Rev. Letters* 30 (1973) 610; *Solid State Commun.* 15 (1974) 1491.
- [43] G. Doyen, Thesis Univ. München (1975).
- [44] H. Conrad, G. Ertl, J. Küppers and E.E. Latta, *Sixth Intern. Congr. on Catalysis*, London, 1976 (to be published).
- [45] B. Feuerbacher and B. Fitton, *Phys. Rev.* B8 (1973) 4890;
B. Feuerbacher, *Surface Sci.* 47 (1975) 115.
- [46] T. Toya, *J. Res. Inst. Catalysis, Hokkaido Univ.* 6 (1958) 308; 8 (1960) 209; 10 (1962) 236.
- [47] T.B. Grimley, *Proc. Phys. Soc. London* 90 (1967) 751.
- [48] T.L. Einstein and J.R. Schrieffer, *Phys. Rev.* B7 (1973) 3629.
- [49] T.B. Grimley and M. Torrini, *J. Phys.* C6 (1973) 868.
- [50] Y. Ebisuzaki, W.J. Kass and M. O'Keeffe, *J. Chem. Phys.* 49 (1968) 3329.
- [51] J.E. Demuth and T.N. Rhodin, *Surface Sci.* 45 (1974) 249.
- [52] D.L. Adams, *Surface Sci.* 42 (1974) 12.